Investigating Bi_2O_3-B_2O_3-BaO Glass Systems for Radiation Shielding Applications

Mergim Gülmen[1*] and Yaşar Bükte[2]

[1]Department of Nuclear Medicine, Ümraniye Training and Research Hospital, 34764 Ümraniye, İstanbul, Turkey
[2]Department of Radiology, Ümraniye Training and Research Hospital, 34764 Ümraniye, İstanbul, Turkey

[*]Corresponding author: mggulmen@gmail.com

ABSTRACT: *This research was conducted to study x-ray and gamma radiation shielding parameters such as mass attenuation coefficient, mean free path, half value layer, tenth value layer, effective atomic numbers, effective electron density for the xBi_2O_3-$(95-x)B_2O_3$-$5BaO$ (where x = 20 mol%, 35 mol%, 50 mol%, and 70 mol%) glass systems with different molar composition. The studied ceramic specimens were denoted by BB20, BB35, BB50 and BB70 and their density values were 4.438 g/cm³, 5.973 g/cm³, 7.156 g/cm³, and 8.005 g/cm³, respectively. Radiation shielding parameters of the samples were investigated by using web based XCOM programme. The obtained results revealed that the highest mass attenuation coefficients were reported for BB70 sample, which has the highest Bi_2O_3 additive in its chemical structure. At 7 MeV photon energy, half value layer (HVL) values were reported as 5.7812 cm, 3.8065 cm, 2.8533 cm, and 2.2457 cm for BB20, BB35, BB50 and BB70, respectively. Therefore, It can be concluded that the present bismuth sesquioxide based glasses in the Bi_2O_3-B_2O_3-BaO glass system have a good quality in radiation protection purposes. Therefore, this glass system can be used as an alternative to conventional materials with the right molar compositon in its chemical formation.*

Keywords: radiation shielding, XCOM, bismuth sesquioxide, bismuth-boron-barium glass, radiation

1.   INTRODUCTION

Development of new methods in the use of ionising radiation for medical purposes have a direct influence on increasing risk in the environment. In this regard radiation protections obligatory condition for the medical centres as well as all the places that radiation uses involved. Although concrete and lead have been primarily used at radiation facilities as a shielding material, they have such disadvantages owing to their high mass, toxicity, and mechanical strenght, causing secondary ionisation and so on. Therefore, for the effective use of the ionising radiation, variety of shielding equipments for instance glasses, alloys and polymers have been reported for the prevention of hazardous effects of high radiation exposure.[1–5] Among them, glasses have drawn attention in terms of their transparency, flexibility, low cost, etc.[6–8]

Heavy metal oxide (such as Bi_2O_3 and PbO) based glasses have been extensively investigated due to their optical properties.[9–10] Bi_2O_3 are highly be demanded in the use of radiation shielding because of its higher refractive index and density, large third-order nonlinear optics susceptibility.[11–13] Embedding different types of oxides like boron oxide and lead oxide into a glass structure promotes its mechanical endurance, thermal disturbance, and chemical distress.[14–16] Glasses which have higher atomic number (Z) or heavy metal oxides enable better quality in radiation protection properties.[17] Lead and lead oxide glasses are in the use of radiodiagnostic purposes at different radiation facilities to protect staff from the high exposure.[18–19] In this study, the x-ray and gamma ray shielding parameters, such as the linear attenuation coefficients (μ), the mass attenuation coefficient (μ/ρ), the half value layer (HVL), the mean free path (MFP), the tenth value layer (TVL), the effective atomic number (Z_{eff}) and the effective electron density (n_{eff}) were studied for the xBi_2O_3-(95-x)B_2O_3-5BaO glass system (where x = 20 mol%, 35 mol%, 50 mol% and 70 mol%).

2.   METHODS

For the present study, a group of Bi_2O_3-B_2O_3-BaO glasses, published by Egorysheva and coworkers were studied in terms of their shielding properties by using XCOM software. The studied glass samples are formulated as xBi_2O_3-(95-x)B_2O_3-5BaO (where x = 20 mol%, 35 mol%, 50 mol% and 70 mol%).[20] Composition (mol%) of the prepared glasses, densities and fraction of elements in the glass composition are exhibited in Table 1.

Table 1: Composition of the studied glasses (mol%), densities and fraction of elements in the chemical formation.

Code	Fraction (mol%)				Faction of elements in each sample			
	Bi_2O_3	B_2O_3	BaO	(g/cm³)	Bi	Ba	B	O
B20	20	75	5	4.438	0.179398	0.044783	0.232928	0.542891
B35	35	60	5	5.973	0.313946	0.044783	0.186343	0.454928
B50	50	45	5	7.156	0.448495	0.044783	0.139757	0.366966
B70	70	25	5	8.005	0.627893	0.044783	0.077643	0.249682

2.1   Mass attenuation coefficients

When a monochoromatic x-ray beam traverses a homogenous object with absorption coefficient μ, the attenuated intensity of the x-ray beams is related to thickness of the object and the ray is described by Lambert's Beer equation:

$$I = I_0 e^{-\mu x}$$ (1)

where I_0 is the x-ray intensity of the x-ray source, I is for the transmitted x-ray intensity, μ is the linear attenuation coefficient and x is the thickness of the studied object.[21] The mass attenuation parameter (μ/ρ) is simply defined as the linear attenuation per unit density of the object (cm²/g).

In this study, μ/ρ values were calculated by using XCOM web based programme.[22]

2.2 Z_{eff} and n_{eff}

The Z_{eff} is the term that is used for complex compound formation. Z_{eff} basically is the number of total electrons in a composite participates in photon-atom interaction.[23] It allows many characteristics like shielding performance of a material to be represented with a number. The Z_{eff} and n_{eff} depends on the total molecular cross-section (σ_t) and total electronic cross-section (σ_e).[24,25] Z_{eff} and n_{eff} can be calculated from the following equations:

$$\sigma_t = \frac{1}{N_A} \sum_i f_i N_i \left(\frac{\mu}{\rho}\right)_i$$ (2)

$$\sigma_e = \frac{1}{N_A} \sum_i \frac{f_i N_i}{Z_i} \left(\frac{\mu}{\rho}\right)_i$$ (3)

$$Z_{eff} = \frac{\sum_i f_i A_i \left(\frac{\mu}{\rho}\right)_i}{\sum_j f_j \frac{A_j}{Z_j} \left(\frac{\mu}{\rho}\right)_j} \tag{4}$$

where f_i, N_i and Z_i represent the fractional abundance, the atomic weight and the atomic number of the element i[th], respectively.

Once Z_{eff} is known, n_{eff} now can be calculated by using the Z_{eff} parameter:

$$n_{eff} = N_A \frac{Z_{eff}}{<A>} \tag{5}$$

2.3   HVL, TVL, and MFP

HVL is the thickness of a homogenous absorber that attenuates the beam intensity to one-half of the original intensity and depends only on the linear attenuation coefficient.[26] The HVL values of the investigated glass samples are determined from the equation:

$$HVL = \frac{\ln(2)}{\mu} \tag{6}$$

The TVL is the thickness of a homogenous absorber which attenuates the beam intensity to one-tenth of the original intensity. TVL values as a radiation protection parameter are used to determine shileding calculations of the treatment rooms. It is computed by,

$$TVL = \frac{\ln(10)}{\mu} \tag{7}$$

MFP is the average distancewhere a photon energy hv travels through an absorber before involving an interaction and it is calculated from the equation:[26]

$$MFP = \frac{1}{\mu} \tag{8}$$

In this study, data were obtained without any personal information regarding the subjects, therefore there was no conflict with the ethical guidelines for clinical research.

3.   RESULTS

In this study, four glasses with different mol compositions which is formulated as the xBi$_2$O$_3$-(95-x)B$_2$O$_3$-5BaO (where x = 20 mol%, 35 mol%, 50 mol% and 70 mol%) were investigated considering their ionising radiation attenuation properties. The densities of the studied glasses were reported as 4.438 g/cm^3, 5.973 g/cm^3, 7.156 g/cm^3 and 8.005 g/cm^3, respectively. In this regard, mass attenuation coefficients (μ/ρ) of the samples were determined in a photon energy range i.e., from 0.015 MeV–15 MeV by using XCOM programme (see Table 2). The variation of μ/ρ againts all the photon energies is depicted in Figure 1.

Table 2: The mass attenuation coefficients (μ/ρ) obtained from XCOM programme.

| Energy (MeV)	BB20	BB35	BB50	BB70
0.015	24.7500	40.1700	55.9500	76.1500
0.02	17.9100	29.8700	41.8200	57.7600
0.03	6.3510	10.5500	14.7500	20.3400
0.04	3.9650	5.9460	7.9260	10.5700
0.05	2.2750	3.3760	4.4770	5.9440
0.06	1.4600	2.1400	2.8200	3.7270
0.08	0.7553	1.0730	1.3910	1.8140
0.1	1.2440	1.1996	2.7480	3.7500
0.2	0.2971	0.4200	0.5428	0.7066
0.3	0.1642	0.2062	0.2483	0.3043
0.4	0.1211	0.1407	0.1604	0.1866
0.5	0.1003	0.1112	0.1220	0.1365
0.6	0.0879	0.0945	0.1011	0.1099
0.8	0.0730	0.0758	0.0787	0.0825
1	0.0639	0.0652	0.0666	0.0684
1.5	0.0509	0.0512	0.0515	0.0519
2	0.0440	0.0444	0.0448	0.0454
3	0.0365	0.0376	0.0386	0.0401
4	0.0326	0.0343	0.0359	0.0382
5	0.0302	0.0324	0.0346	0.0376
6	0.0287	0.0314	0.0341	0.0376
7	0.0277	0.0308	0.0339	0.0380
8	0.0270	0.0305	0.0339	0.0386
9	0.0266	0.0304	0.0342	0.0392
10	0.0263	0.0304	0.0345	0.0399
15	0.0259	0.0313	0.0366	0.0438
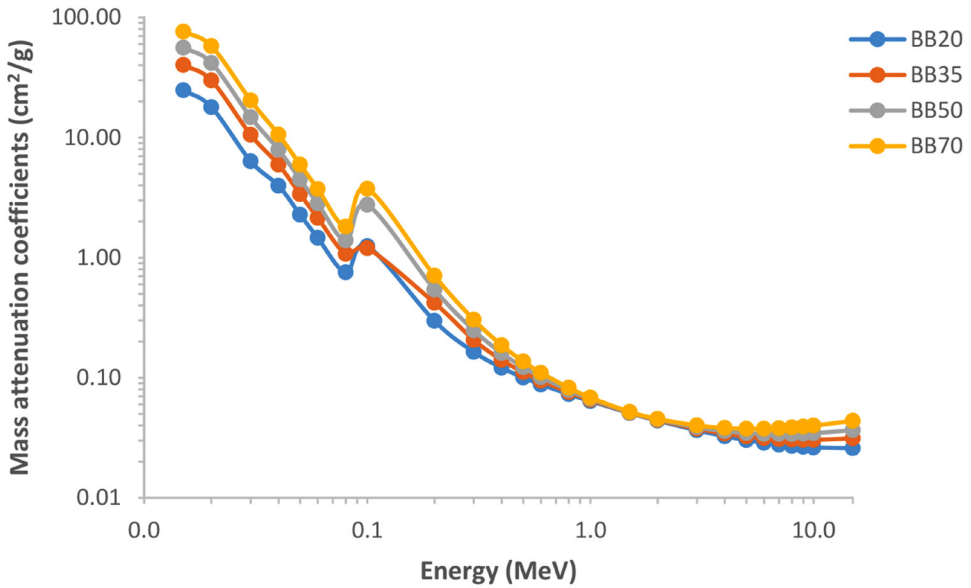
Figure 1:   The variation of mass attenuation coefficients against photon energy for all glasses.

For the energies E < 0.1 MeV, μ/ρ values decrease rapidly for all samples, however there is a peak observed around 80 keV–100 keV due to the photoelectric dominancy in this energy range. At these uncharacteristically high values of μ/ρ, the photon energies were just above the binding energy of the orbital electrons within the atoms resulting in substantially enhanced probability of photon interaction via photoelectric effect at these particular energies. The compositions which include Bi atoms enhanced the probabilities of interaction between the incident photons and the orbital electrons of the sample via photoelectric effect, compton inelastic scattering and pair production (note that pair production takes place only at photon energies grater than the rest mass energy of an electron-positron pair) due to its high Z and ρ values. The relationships between the cross sections for each mechanism and its photon/material characteristics are $\sigma_{pe}\alpha Z_n/(h\nu)^3$, $\sigma_{com}\alpha\ 1/n_e$, $\sigma_{pp}\alpha Z^2$, where σ_{pe} is the photoelectric cross-section, σ_{com} is the compton scattering cross-section, σ_{pp} is the pair production cross-section, Z is the atomic number, h is the Planck's constant, ν is the frequency of the incident photon, and n_e is the electron density.[27] It can be concluded from the Figure 1 that μ/ρ values decreased with increasing photon energy by the link of μ from the Beer-Lambert equation (see Equation 1). It is also found that the increasing molar weight of Bi_2O_3

additive increased the μ/ρ values systematically (see Table 2). The highest value of μ/ρ occured for BB70 sample which has the highest molar weight of Bi_2O_3 additive. The similar results can be found in literature.[28–32] There are many studies in literature where XCOM results were in good agreement with other codes such as Monte Carlo in calculating mass attenuation coefficient.[35–38] The lower half value layer values are required for better radiation protection among the investigated shielding materials.[33,34] The results from the HVL values of the glass samples are depicted in Figure 2.
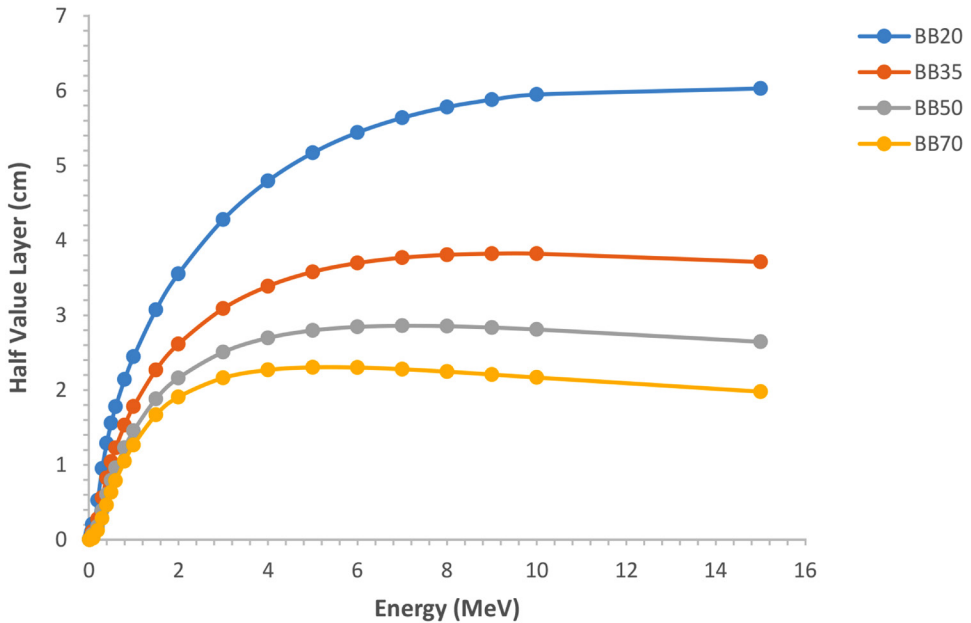

Figure 2: The variation of HVL against photon energy for all glasses.

According to inverse relationship between HVL and values (see Equation 6), it can be concluded that lower HVL values can be achieved by higher values. Among the glasses, BB70 has the lowest HVLs against the photon energy range. This can be attributed to higher values of BB70 over others. Moreover, it can be seen from the results that BB70 requires less shielding thickness due to the difference between HVLs of the glasses, paticularly at high energies. A similar concept related to radiation shielding parameters is the TVL. TVL is also quantitative raw factor for characterisation of the radiation travelling through a given object. The variation of TVL values against all photon energies is depicted in Figure 3.
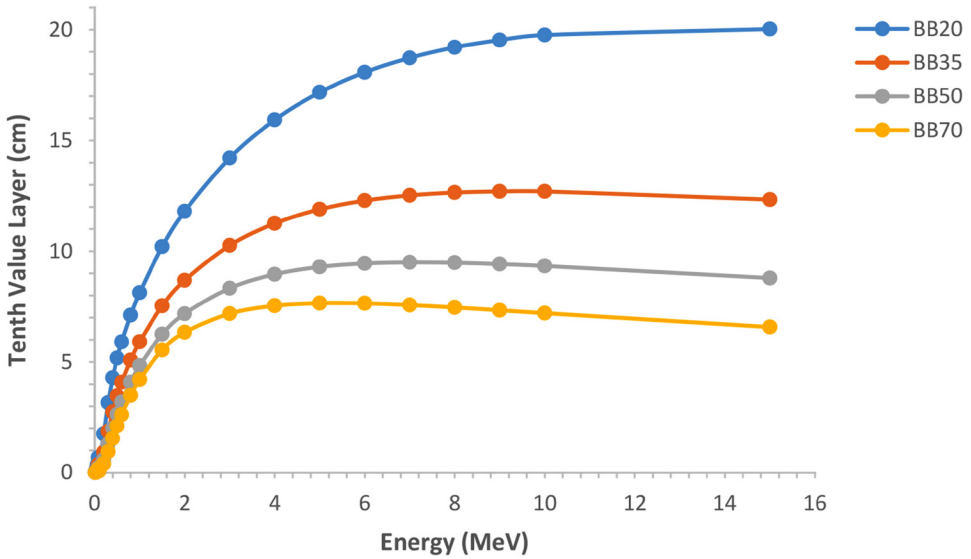
Figure 3: The TVL against photon energy for all glasses.

It can be seen from the graph that the trendis the same as HVLs for the same energy range. The minimum TVL values were reported for BB70 glass sample. Besides, at maximum photon energy (15 MeV), TVLs were calculated from the equation (7) as 20.0322 cm, 12.3320 cm, 8.7867 cm, and 6.5732 cm for BB20, BB35, BB50, and BB70, respectively. While the concentration of Bi_2O_3 was increased from 20 mol%–70 mol%, the TVLs for BB70 was decreased in the amount of 67.2%. The glass samples were also investigated in terms of their mean free path parameters and the findings are depicted in Figure 4.

BB70 sample has the lower MFP values among others. The behaviour of MFP values have similar trend to the HVLs since they are both inversely proportional to the linear attenuation coefficient. Effective atomic numbers were calculated as well and the results from the Z_{eff} values for all photon energies can be seen in Figure 5.
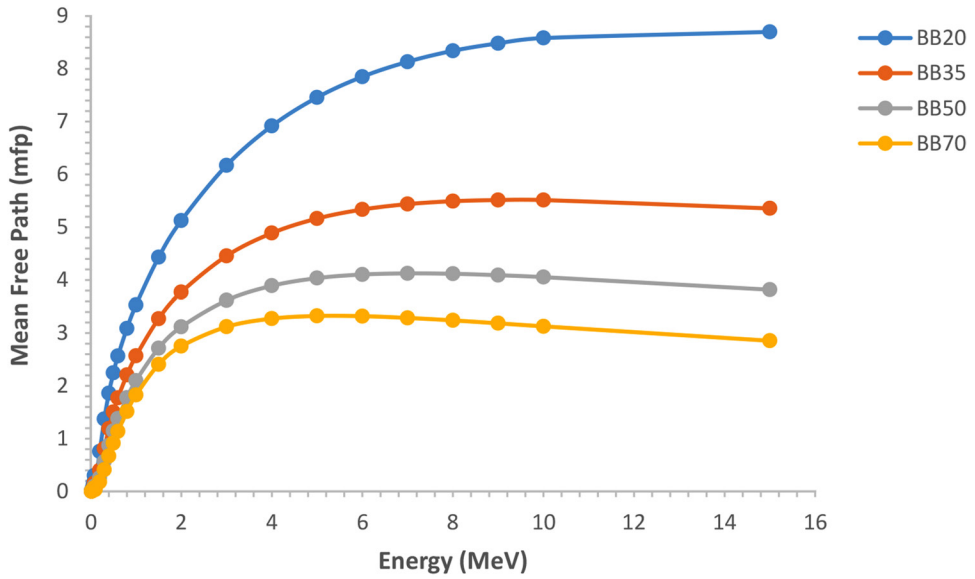
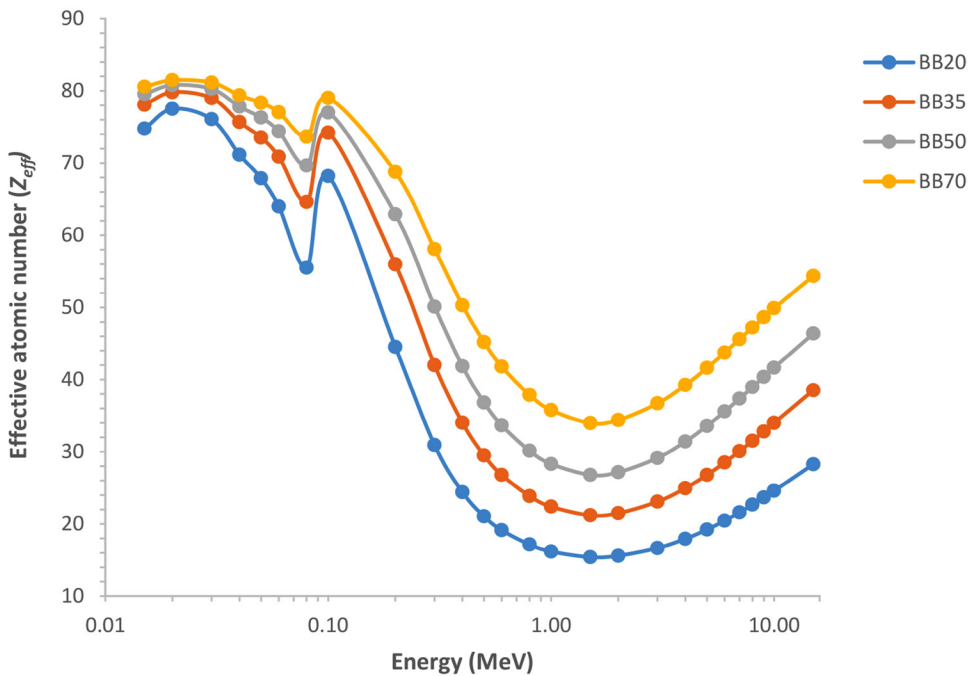Figure 4: The variation of MFP against photon energy for all glasses.

Figure 5: The variation of Z_{eff} against photon energy for all glasses.

The findings from the Z_{eff} agrees with the μ/ρ values. One can see clearly from Figure 5, Z_{eff} has jumps in the lower photon energy range owing to absorption edge effects of high elements. The Z_{eff} values decrease sharply with increasing photon energy at the region of 100 keV–2 MeV in which the probability of photoelectric effect decreases and compton effect becomes dominant process. The change in effective atomic number with different compositions was very large between the samples. Higher Z_{eff} values of BB70 glass sample imply that gamma photons are more probable to be absorbed because of the high molar content with the high atomic number of Bi. Therefore, it can be concluded that BB70 sample has better attenuation properties according to the results from μ/ρ and Z_{eff} values. The term n_{eff} for studied samples were also evaluated by using equation (5). The results are depicted in Figure 6. Highest n_{eff} values were found for BB70 glass as expected because of its high effective atomic number.
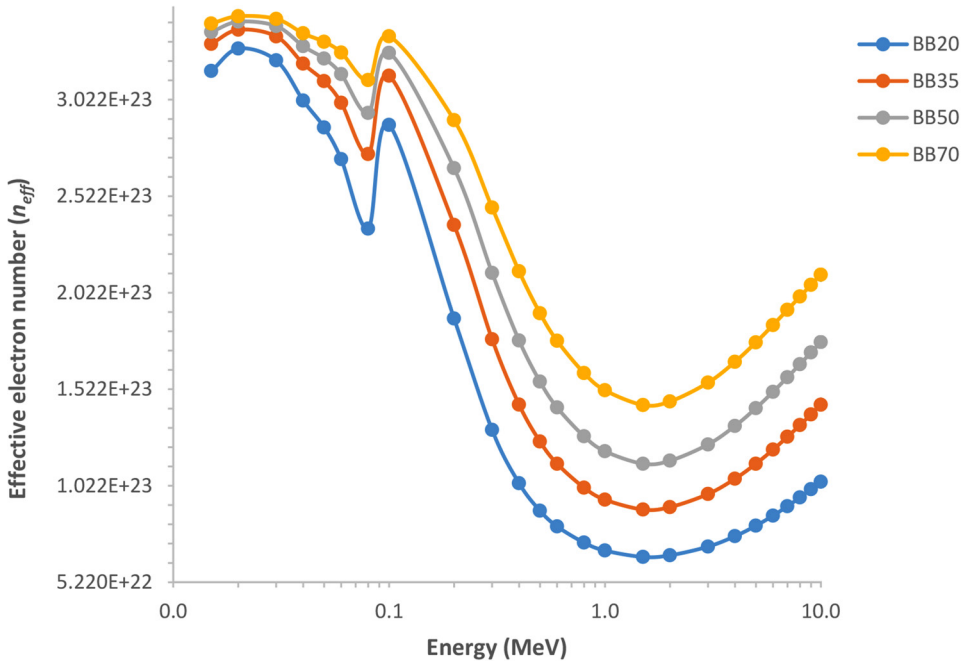

Figure 6: The variation of n_{eff} against photon energy for all glasses.

4. DISCUSSION

The research article is presented on the basis of radiation shielding properties for the xBi$_2$O$_3$-(95-x)B$_2$O$_3$-5BaO (where x = 20 mol%, 35 mol%, 50 mol% and 70 mol%). The studied specimens were denoted by BB20, BB35, BB50 and BB70, and their density values were 4.438 g/cm^3, 5.973 g/cm^3, 7.156 g/cm^3 and 8.005 g/cm^3, respectively. The radiation protection parameters of the present glasses were investigated with different molar composition of Bi$_2$O$_3$ and B$_2$O$_3$ substitutions. It was deduced that the highest μ/ρ values were found for BB70 glass sample, which has the highest Bi$_2$O$_3$ additive in its chemical formation. The minimum HVLs and TVLs were recorded for BB70 glasses. At the highest photon energy (15 MeV), TVL values were calculated as 20.0322 cm, 12.3320 cm, 8.7867 cm and 6.5732 cm for BB20, BB35, BB50 and BB70, respectively. It is also found that the HVL and MFP values of the studied samples were proportionally increased with the increasing photon energy, which is the indication of the stong attenuation of the photon intensity of the glasses. The highest values of Z_{eff}, such as 77.51, 79.82, 80.80, 81.47 were recorded at 0.02 MeV photon energy for BB20, BB35, BB50 and BB70 samples, respectively. Therefore, it can be concluded that the present bismuth sesquioxide based glasses have a good quality in radiation protection purposes. The molar composition of elements in the chemical composition is also a key factor for better radiation shielding properties.

5. REFERENCES

1. Kaur, T., Sharma, J. & Singh, T. (2017). Thickness optimization of Sn–Pb alloys for experimentally measuring mass attenuation coefficients. *Nucl. Energy Technol.*, 3(1), 1–5. https://doi.org/10.1016/j.nucet.2017.02.001

2. Mirji, R. & Lobo, B. (2017). Computation of the mass attenuation coefficient of polymeric materials at specific gamma photon energies. *Radiat. Phys. Chem.*, 135, 32–44. https://doi.org/10.1016/j.radphyschem.2017.03.001

3. Kaewjaeng, S. et al. (2012). Effect of BaO on optical, physical and radiation shielding properties of SiO$_2$-B$_2$O$_3$-Al$_2$O$_3$-CaOe-Na$_2$O glasses system. *Process Eng.*, 32, 1080–1086. https://doi.org/10.1016/j.proeng.2012.02.058

4. Singh, K. J., Kaur, S. & Kaundal, R. S. (2014). Comparative study of gamma ray shielding and some properties of PbO-SiO$_2$-Al$_2$O$_3$ and Bi$_2$O$_3$-SiO$_2$-Al$_2$O$_3$ glass systems. *Radiat. Phys Chem.*, 96, 153–7. https://doi.org/10.1016/j.radphyschem.2013.09.015

5. Ersundu, A. E. et al. (2018). The heavy metal oxide glasses within the WO$_3$-MoO$_3$-TeO$_2$ system to investigate the shielding properties of radiation applications. *Prog. Nucl. Energy*, 104, 280–287. https://doi.org/10.1016/j.pnucene.2017.10.008

6.   Kirdsiri, K. et al. (2011). Comparative study of silicate glasses containing Bi_2O_3, PbO and BaO: Radiation shielding and optical properties. *Ann. Nucl. Energy*, 38(6), 1438–1441. https://doi.org/10.1016/j.anucene.2011.01.031

7.   Dong, M. G. et al. (2017). Investigation of gamma radiation shielding properties of lithium zinc bismuth borate glasses using XCOM program and MCNP5 code. *J. Non-Cryst. Solids*, 468, 12–16. https://doi.org/10.1016/j.jnoncrysol.2017.04.018

8.   Sayyed, M. I., Qashou, S. I. & Khattari, Z. Y. (2017). Radiation shielding competence of newly developed TeO_2-WO_3 glasses. *J. Alloy. Comp.*, 696, 632–638. https://doi.org/10.1016/j.jallcom.2016.11.160

9.   Knoblochova, K. et al. (2009). Raman spectra and optical properties of selected Bi_2O_3-PbO-B_2O_3-GeO_2 glasses. *Opt. Mater.*, 31(6), 895–898. https://doi.org/10.1016/j.optmat.2008.10.024

10.   Golis, E. P. & Ingram, A. (2007). Investigations of magneto-optic properties in PbO–Bi_2O_3–GeO_2 glass system. *J. Phys. Conference Series*, 79, 012003. https://doi.org/10.1088/1742-6596/79/1/012003

11.   Hasegawa, T. (2011). Optical Properties of Bi_2O_3–TeO_2–B_2O_3 Glasses. *J. Non Cryst. Solids*, 357(15), 2857–2862. https://doi.org/10.1016/j.jnoncrysol.2011.03.021

12.   Rao, L. S. et al. (2012). Optical properties of alkaline earth borate glasses. *Int. J. Eng, Sci. Technol.*, 4(4),25–35. https://doi.org/10.4314/ijest.v4i4.3

13.   Nasu, H. et al. (1996). Third-order optical non-linearity of Bi_2O_3-based glasses. *Non-Cryst. Solids,* 204, 78–82. https://doi.org/10.1016/0022-3093(96)00395-X

14.   Safeya, I., Abdel-Baki, M. & El-Diasty, F. (2012). Zinc borophosphate glasses for infrared-based optical applications. *Opt. Eng.*, 51(9), 093401. https://doi.org/10.1117/1.OE.51.9.093401

15.   Rinke, M. T. & Eckert, H. (2011). The mixed network former effect in glasses: solid state NMR and XPS structural studies of the glass system $(Na_2O)(x)(BPO_4)$ (1–x). *Phys. Chem. Chem. Phys.*, 13(14), 6552–6565. https://doi.org/10.1039/c0cp01590c

16.   Sdiri, N. et al. (2015). Structural investigation of amorphous Na_2O–P_2O_5–B_2O_3 correlated with its ionic conductivity. *J. Non Cryst. Solids*, 409, 34–42. https://doi.org/ 0.1016/j.jnoncrysol.2014.11.009

17.   Tekin, H. O. et al. (2019). Photon and neutron shielding performance of boron phosphate glasses for diagnostic radiology facilities. *Results in Physics*, 12, 1457–1464. https://doi.org/10.1016/j.rinp.2019.01.060

18.   Sava, B. A. et al. (2017). Bismuth and lead oxides codoped boron phosphate glasses for Faraday rotators. *Ceram. Int.*, 44(6), 6016–6025. https://doi.org/10.1016/j.ceramint.2017.12.205

19.   Morishima, Y., Chida, K. & Meguro, T. (2018). Effectiveness of additional lead shielding to protect staff from scattering radiation during endoscopic retrograde cholangiopancreatography procedures. *J. Radiat. Res.*, 59(2), 225–232. https://doi.org/10.1093/jrr/rrx039

20.   Egorysheva, A. V., Volodin, V. D. & Skorikov, V. M. (2008). Glass Formation in the Bi$_2$O$_3$–B$_2$O$_3$–BaO System. *Inorganic Materials*, 44(11), 1261–1265. https://doi.org/10.1134/S0020168508110228

21.   Maier, A. et al. (2018). *Medical imaging systems: an introductory guide*, 1st ed. Switzerland: Springer, 127–128. https://doi.org/10.1007/978-3-319-96520-8

22.   Berger, M. J. & Hubbel, J. H. (1999). *XCOM: Photon cross sections database, web version 1.2.* Originally Published as NBSIR 87-3597 XCOM: Photon Cross Sections on a Personal Computer, Washington, DC. Retrieved 8 June 2021 from http://physics.nist.gov/xcom

23.   Hosamani, M. M. & Badiger, N. M. (2018). Determination of effective atomic number of composite materials using backscattered gamma photons – a novel method. *Chem. Phys. Lett.*, 695, 94–98. https://doi.org/10.1016/j.cplett .2018.02.012

24.   Wang, D. C., Ping. L. A & Yang, H. (1995). Measurement of the mass attenuation coefficients for SiH4 and Si. *Nucl. Instr. Meth. B.*, 95, 161–165.

25.   Singh, K. et al. (2002). Gamma-ray attenuation coefficients in bismuth borate glasses. *Nucl. Instr. Meth. B.*, 194, 1–6. https://doi.org/10.1016/S0168-583X(02) 00498-6

26.   Podgorsak, E. B. (2005). *Radiation physics for medical physicists*. 2nd ed. New York: Springer, 282–283. https://doi.org/10.1007/978-3-642-00875-7

27.   Hirayama, H. (2000). Lecture note on photon interactions and cross sections. *KEK Internal*, 2000–2010. Retrieved 1 February 2021 from http://rcwww.kek .jp/research/shield/photon_r.pdf

28.   AlBuriahi, M. S. et al. (2021). Effect of CdO addition on photon, electron, and neutron attenuation properties of boro-tellurite glasses. *Ceram. Int.*, 47(5), 5951–5958. https://doi.org/10.1016/j.ceramint.2020.10.168

29.   Divina, R. et al. (2020). Effect of different modifier oxides on the synthesis, structural, optical, and gamma/beta shielding properties of bismuth lead borate glasses doped with europium. *J. Mater. Sci: Mater Electron*, 31(23), 21486– 21501. https://doi.org/10.1007/s10854-020-04662-3

30.   Al-Buriahi, M. S. et al. (2021). Polarizability, optical basicity, and photon attenuation properties of Ag$_2$O–MoO$_3$–V$_2$O$_5$–TeO$_2$ glasses: The role of silver oxide. *J. Inorg. Organomet. Polym.*, 31(3), 1047–1056. https://doi.org/10.1007/ s10904-020-01750-z

31.   Al-Buriahi, M. S. et al. (2020). Effect of chromium oxide on the physical, optical, and radiation shielding properties of lead sodium borate glasses. *J. Non-Cryst. Solids*, 544, 120171. https://doi.org/10.1016/j.jnoncrysol.2020.120171

32.   Alajerami, Y. S. et al. (2020). Radiation shielding properties of bismuth borate glasses doped with different concentrations of cadmium oxides. *Ceram. Int.*, 2020, 46(8B), 12718–12726.

33.   Almatari, M. (2019). Gamma radiation shielding properties of glasses within the TeO$_2$-TiO$_2$-ZnO system. *Radiochim. Acta*, 107(6), 517–522. https://doi.org/ 10.1515/ract-2018-3058

34. Kaundal, R. S. (2016). Comparative study of radiation shielding parameters for bismuth borate glasses. *Mat. Res*., 19(4), 776–780. https://doi.org/10.1590/1980-5373-MR-2016-0040

35. Bagheri, R., Moghaddam, A. K. & Yousefnia, H. (2017). Gamma ray shielding study of barium–bismuth–borosilicate glasses as transparent shielding materials using MCNP-4C code, XCOM program, and available experimental data. *Nucl. Eng. and Technol*., 49(1), 216–223. https://doi.org/10.1016/j.net.2016.08.013

36. Shirmardi, S. P., Shamsaei, M. & Naserpour, M. (2013). Comparison of photon attenuation coefficients of various barite concretes and lead by MCNP code, XCOM and experimental data. *Ann. Nucl. Energy*, 55, 288–291. https://doi.org/10.1016/j.anucene.2013.01.002

37. Sayyed, M. I. et al. (2018). Radiation shielding parameters of $BaO–Nb_2O_5–P_2O_5$ glass system using MCNP5 code and XCOM software. *Mater. Res. Express*, 5(11), 115203. https://doi.org/10.1088/2053-1591/aaddc7

38. Mahmoud, K. A., Sayyed, M. I. & Tashlykov, O. L. (2019). Comparative studies between the shielding parameters of concretes with different additive aggregates using MCNP-5 simulation code. *Radiat. Phys. Chem.*, 165, 108426. https://doi.org/10.1016/j.radphyschem.2019.108426